

AD A 030744

AFATL-TR-76-44

12

THE DESIGN AND CHARACTERIZATION OF AN ALUMINUM FRAGMENT PROJECTOR

VULNERABILITY ASSESSMENTS BRANCH WEAPON SYSTEMS ANALYSIS DIVISION

APRIL 1976

FINAL REPORT: APRIL 1973 - AUGUST 1975

Approved for public release; distribution unlimited

AIR FORCE ARMAMENT LABORATORY

AIR FORCE SYSTEMS COMMAND • UNITED STATES AIR FORCE

EGLIN AIR FORCE BASE, FLORIDA



UNCLASSIFIED

SECURITY CLASSIFICATION OF THIS PAGE (When Data Entered)

REPORT DOCUMENTATION PAGE		READ INSTRUCTIONS BEFORE COMPLETING FORM
1. REPORT NUMBER AFATL-TR-7G-44	2. GOVT ACCESSION NO.	3. RECEIPT'S CATALOG NUMBER
4. TITLE (and Subtitle) THE DESIGN AND CHARACTERIZATION OF AN ALUMINUM FRAGMENT PROJECTOR	5. TYPE OF REPORT & PERIOD COVERED Final Report 2/1 April 1973-August 1975	
7. AUTHOR(s) John F. Black Robert F. Brandt Kevin T. McArdle	6. PERFORMING ORG. REPORT NUMBER	
9. PERFORMING ORGANIZATION NAME AND ADDRESS Weapon System Analysis Division (DLYV) Air Force Armament Laboratory Eglin Air Force Base, FL 32542	10. PROGRAM ELEMENT, PROJECT, TASK AREA & WORK UNIT NUMBERS 2549 03 18	
11. CONTROLLING OFFICE NAME AND ADDRESS Air Force Armament Laboratory Armament Development and Test Center Eglin Air Force Base, FL 32542	12. REPORT DATE April 1976	
14. MONITORING AGENCY NAME & ADDRESS (if different from Controlling Office)	13. NUMBER OF PAGES 43	
	15. SECURITY CLASS. (If this report) UNCLASSIFIED	
	16. DECLASSIFICATION/DOWNGRADING SCHEDULE	
16. DISTRIBUTION STATEMENT (of this Report) Approved for public release; distribution unlimited		
17. DISTRIBUTION STATEMENT (of the abstract entered in Block 20, if different from Report)		
18. SUPPLEMENTARY NOTES Available in DDC		
19. KEY WORDS (Continue on reverse side if necessary and identify by block number) Explosive Fragment Projector Flash Panels Aluminum Fragments Flash X-ray Depth of Penetration Aerodynamic Fragment Drag Dahlgren Screens Warhead Characterization		
20. ABSTRACT (Continue on reverse side if necessary and identify by block number) An explosive fragment projector that launches 32, 2.26-gram aluminum cubes at a maximum initial speed of 10,000 ft/sec within a solid angle of 3 milliradians is described. Various characterization techniques are discussed.		

UNCLASSIFIED

SECURITY CLASSIFICATION OF THIS PAGE (When Data Entered)

UNCLASSIFIED

SECURITY CLASSIFICATION OF THIS PAGE (When Data Entered)

PREFACE

This report documents an Air Force Armament Laboratory in-house effort under Project 2549 03 18. The tests were conducted at Range C-64A from 9 April 1973 to 7 August 1975.

Dr. Kevin T. McArdle, DLYW was the program manager.

This report has been reviewed by the Information Office (OI) and is releasable to the National Technical Information Service (NTIS). At NTIS, it will be available to the general public, including foreign nations.

This technical report has been reviewed and is approved for publication.

FOR THE COMMANDER

J. R. MURRAY
Chief, Weapon Systems Analysis Division



¹
(The reverse of this page is blank)

TABLE OF CONTENTS

Section	Title	Page
I	INTRODUCTION	1
II	DESIGN SELECTION TESTS	2
	1. End Projector Tests	2
	2. Dished Mat Projector Tests	2
	3. Plastic Filled Mat Projector	3
III	DETAILED CHARACTERIZATION TESTS OF PLASTIC-FILLED PROJECTOR	4
	1. Fragment Mass Distribution	4
	2. Fragment Speed Distribution	4
	3. Fragment Spatial Distribution	6
	4. Comparison of Characterization Methods	6
IV	CONCLUSIONS	8
References		35
Appendix		
A	COMPUTATION METHODS	37

LIST OF FIGURES

Figure	Title	Page
1	End Projector	9
2	Fragment Spatial Distribution at 24 Feet	10
3	Dished Mat Projector	11
4	Witness Panel Impacts at 24 Feet, Shot Number 30 . . .	12
5	Cross Section of Plastic Filled Mat Projector	13
6	Witness Panel Impacts at 24 Feet, Shot 44	14
7	Number of Recovered Fragments by Mass Class	15
7	Number of Recovered Fragments by Mass Class (Continued)	16
7	Number of Recovered Fragments by Mass Class (Concluded)	17
8	Number of Recovered Fragments at 48 Feet by Mass Class	18
9	Average Number of Fragments at 48 Feet by Mass Class	19
10	Comparison of Speed Measurement Techniques	20
10	Comparison of Speed Measurement Techniques (Continued)	21
10	Comparison of Speed Measurement Techniques (Concluded)	22
11	Shot Distribution by Dahlgren Screens	23
12	Shot Distribution by Depth of Penetration	24
13	Initial Speed Distribution by Depth of Penetration . .	25
14	Plan View of X-ray Set Up	26
15	Initial Speed Distribution by Flash X-ray	27
16	Fragment Spatial Distributions	28
16	Fragment Spatial Distributions (Concluded)	29
17	Average Fragment Spatial Distribution	30

LIST OF TABLES

Table	Title	Page
1	Dished Mat Projector Results	31
2	Properties of Aluminum Filled Plastic	32
3	Design Parameters and Results	33
4	Final Design Performance	34

SECTION I
INTRODUCTION

The objective of this effort was to develop an explosive device capable of projecting 32, 2.26-gram aluminum cubes^a at an initial speed of 10,000 ft/sec within a solid angle of 3 millisteradians. An experimental approach to the design was taken. The designs were checked by testing prototype models for fragment spatial distribution and fragment speed by using high speed cameras to record impact flashes on steel witness panels. The final design underwent more extensive characterization testing using fiberboard recovery bundles, flash X-rays and Dahlgren (Reference 1) screens.

Footnote

^aThe aluminum projectiles were not exactly cubical, but had nominal dimensions of 0.375x0.375x0.355 inch.

SECTION II

DESIGN SELECTION TESTS

The designs tested can be divided into three types of devices. Each type will be discussed and results presented in the order in which it was tested.

1. END PROJECTOR TESTS

Items of the first type were end projectors designed and supplied by DLJW, the Warheads and Explosives Branch. The basic device is illustrated in Figure 1. Other variations of the device included the use of plastic and metal wave shaping cones embedded in the explosive, and concentric lead sleeves surrounding the fragment end of the cylinder. These projectors were tested for spatial and speed distributions by firing them at 0.020-inch-thick steel panels at a standoff of 24 feet. The flashes due to fragment impacts were recorded by high speed cameras.

Figure 2 illustrates the spatial distribution of the fragments at a distance of 24 feet from the point of detonation for a projector of this type with a concave end. Assuming it was a whole cube,^a the initial speed of the first arrival for this firing was 11,300 ft/sec.^a The spatial distribution and speed are typical of those obtained for devices of this type. While use of the lead sleeves and/or concave ends did show a slight improvement in the spatial distribution of fragments, it became apparent that the item could not be improved sufficiently and the design was abandoned.

2. DISHED MAT PROJECTOR TESTS

The second type of device, designed by DLRD, the Terminal Ballistics Branch, employed a much smaller length to diameter ratio and had the fragments mounted in a concave face. In addition, the explosive charge was initiated simultaneously around the perimeter. The design is illustrated in Figure 3. The explosive charge was handcrafted in the field from standard 1.25-pound blocks of composition C4.

Figure 4 illustrates the fragment pattern produced at 24 feet by the first item of this type tested. All impacts on the steel witness panel were within a 32-inch diameter circle (9.7 millisteradians). A series of tests was then conducted in which the thicknesses L and T, the radius R, and diameter D were varied. Design parameters and firing results for

Footnote

^aSee Equation (11) of Appendix A for details of the determination of initial speeds.

items of this type are listed in Table 1. All items of this type produced fragment patterns with less dispersion than items of the end projector type.

3. PLASTIC FILLED MAT PROJECTOR

While the fragment spatial distributions of the dished mat projectors were close to the design goal, the highest speed obtained was 1500 ft/sec below that required. Difficulties encountered in fabricating the concave surface by hand implied that any final model would require a cast explosive fill. In addition, those projectors with thicknesses such that a large amount of explosive remained behind the central cubes, produced extensive breakup of the cubes.

At this point in the development, a serendipitous change in the design was made. It was noticed that projectors with almost no explosive behind the central cubes were producing acceptable fragment patterns. It was reasoned, and incorrectly so, that the fragment pattern produced by these devices was controlled more by the quantity of explosive directly behind the cubes than by the concavity of the surface. Therefore, a projector with a flat explosive charge having a plug of explosive removed from the center should behave in the same manner as a projector with a deep concave surface. In addition, flat surfaced projectors would be simpler to fabricate by hand. To test this hypothesis a third type projector, as illustrated in Figure 5, was constructed. Notice that in addition to the flat surface and cylindrical cavity in the center of the explosive, the 32 cubes are embedded in a disk of aluminum-filled plastic. Properties of this plastic are given in Table 2.

The fragment spatial distribution at 24 feet for shot 44, which had a maximum initial speed of 8125 ft/sec, is given in Figure 6. The dispersion of the fragment pattern was as small as that of the devices with concave surfaces but the speed was still 2000 ft/sec too low. Subsequent firings of identical projectors without the plastic surrounding the cubes produced fragment patterns with excessive dispersion similar to that of Figure 2.

As the design appeared very promising, a series of firings was conducted that varied the thickness of the explosive charge, the presence or absence of the cylindrical cavity at the center and the presence or absence of the central four aluminum cubes.^a Results of these firings are given in Table 3. From these results, it was determined that a model with a solid disk of explosive 1-inch thick and having the original fragment arrangement was suitable for more detailed characterization tests.

Footnote

^aThe four cubes when removed from the center of the pattern were placed at the corners of the pattern, keeping the total number 32.

SECTION III
DETAILED CHARACTERIZATION TESTS
OF PLASTIC-FILLED MAT PROJECTOR

Table 4 lists the pertinent parameters for 20 characterization tests. Initial speeds listed in this table assume the fastest fragment was a whole cube.

1. FRAGMENT MASS DISTRIBUTION

Fragment mass distributions were obtained by firing the fragment projectors into bundles of 8 x 4 x 2-foot thick fiberboard at standoff distances of 24, 48, and 96 feet. Histograms of the recovered fragment masses are given in Figure 7. A comparison of these histograms indicates that no whole cubes were recovered at 24 feet, and that there are no significant differences between fragments recovered at 48 and 96 feet. The breakup of whole cubes illustrated in histograms (a) and (b) is due to impact on the fiberboard bundles, while the breakup shown in histograms (c), (d), (e), and (f), occurs primarily on launching rather than on recovery of the cubes.

Therefore, fragments recovered in fiberboard at standoffs of 48 feet or greater accurately represent the launched fragment masses. Additional recovered fragment histograms are given in Figure 8.

Figure 9 presents the average of the seven individual 48-foot shots. The vertical bars establish the 1-sigma limits.

2. FRAGMENT SPEED DISTRIBUTION

The distribution of initial fragment speeds was studied by a number of methods: flash panels, Dahlgren screens, depth of penetration, and flash X-ray. Each of these methods has its own peculiarities, making a direct comparison of results difficult.

a. Flash Panel Measurements

Early attempts to obtain fragment arrival times at 24 feet by using high speed cameras (8,000 frames per second) to record impact flashes on steel witness panels were not successful. The brightness, and close spacing of the flashes precluded the identification of impacts other than the first. Tests conducted with the panels at 48 feet were equally unsuccessful. Therefore, usually only the arrival time of the fastest fragments could be determined by this method.

b. Dahlgren Screen Measurements

During the optimization of the design of the projector, attempts were made to obtain fragment arrival times at 24 feet by using Dahlgren screens mounted on the front surface of the fiberboard recovery bundles. The Dahlgren screen system is a make-type circuit which produces an electrical signal whenever a metal fragment passes through the screen. therefore, this method produces a list of fragment arrival times at the screen location. In addition the screens also serve as witness panels, yielding the spatial distribution. However, no information is obtained that associates fragment masses with times of arrival. While this system worked successfully with some projector designs, the final projector design produced a fireball of detonation products that interfered with the operation of the screens, such that only the arrival time of the fastest fragments could be determined. Fortunately, it was discovered during the course of the 48-foot firings for fragment recovery that the fireball did not normally extend that far. This permitted the use of Dahlgren screens to obtain times of arrival at 48 feet.

c. Depth of Penetration Measurements

The results of the firings into fiberboard at 48 feet were also used to calculate impact speeds from the depth of penetration of the fragments into the fiberboard.^a While the speeds calculated by this method have large error limits, the method has the advantage of associating a mass, impact speed, and location with each fragment.

The results obtained by this and the Dahlgren screen method are not directly comparable. The Dahlgren screen method gives arrival times but no masses. This makes a calculation of either the initial or the impact speed impossible. However, as masses are obtained with depth of penetration data, the impact speeds can be converted to equivalent arrival times. This calculation also requires a knowledge of the drag in the air of the aluminum fragments. To make a more appealing comparison the quantity S_{rot} is defined as

$$S_{rot} = \frac{R}{T}$$

where R is the constant radius at which the arrival time T is measured.

Footnote

^aMann barrel firings of aluminum fragments into fiberboard were conducted to determine this relationship. A series of similar firings were also conducted to determine the aerodynamic drag of the aluminum fragments. Detailed results will appear in a future report, while the results are given in Appendix A.

This quantity is often mistakenly referred to as the average velocity. Details of the calculations are given in Appendix A, while the results are illustrated in Figure 10. The average S_{rot} speeds of shots 135, 136, 145, 149 and 152, determined by Dahlgren screens, are presented in Figure 11. The average S_{rot} speeds of the same shots determined by depth of penetration are given in Figure 12. The latter method yields fewer high speed fragments and more slow speed fragments than the former method. The impact speeds determined by depth of penetration have also been converted to initial speeds, and the average initial speeds of shots 135, 136, 145, 149 and 152 are presented in Figure 13.

d. Flash X-Ray Measurements

Flash X-ray techniques were also used to study the speed distribution of the fragments. Figure 14 illustrates the test setup. The large film to head distance and small fragment to film distance minimized parallax effects. The film was exposed when the first fragment impacted the Dahlgren screen. The data obtained in these tests are in the form of fragment positions at the instant of time at which the fastest fragment has traveled 24 feet. Because of the high spatial density of fragments, it was impractical to recover and match fragments with the images on the exposed film. For film images that appeared to be whole or almost whole cubes, the position data were used to calculate initial speeds. In calculating speeds, all fragments were considered as being on a line extending from the initial device location to the center of impact. The maximum error introduced into the initial speeds by this assumption is 150 ft/sec.

The histogram shown in Figure 15 presents the average initial speeds of five such X-ray tests. The 22 fragments included in this histogram are in good agreement with the average number (26) of large fragments recovered in the fiberboard bundles.

3. FRAGMENT SPATIAL DISTRIBUTION

The spatial distribution of the fragments was determined by recording the location of fragment impacts obtained during the flash panel and Dahlgren screen tests at 48-foot standoff. The center of impact was then calculated, and the number of fragments lying in incremental solid angles centered on the center of impact determined. The individual and average results obtained for eight shots are shown in Figures 16 and 17.

4. COMPARISON OF CHARACTERIZATION METHODS

No difficulties were encountered with the determination of the spatial distributions of the fragments from the impacts on the Dahlgren screens, flash panels or fiberboard bundles. When mass distributions are to be obtained by recovery of the fragments from fiberboard, care must be taken to insure that the fragments do not breakup on impacting the fiberboard. A comparison of fragment mass distributions recovered at different

distances will aid in the selection of a suitable recovery distance that minimizes breakup.

The determination of speed distributions presents the most difficulty. Flash panels or Dahlgren screens readily provide time of arrival data. However, given N impacts on either one, the flash panel will provide less than N time of arrival signals while the Dahlgren screen will provide more than N signals. Application of the time of arrival data is also complicated by the fact that each time of arrival signal cannot be identified with a definite mass. This makes calculations of initial speeds impossible. The flash X-ray has the advantage of being the only method to yield measurements of speed over very short path lengths. However, no accurate mass can be associated with each fragment. It is possible to make estimates of the fragment masses from the size of the images on the radiographs, but the estimates are subject to large errors.

As mentioned previously only the technique that employs firings into fiberboard recovery bundles has the advantage of associating a mass, impact speed and location with each fragment.

SECTION IV

CONCLUSIONS

All design goals were met. It is recommended that any similar fragment projectors be characterized by firings into three adjacent fiberboard bundles, 30 sheets thick, at a standoff of 48 feet. The X-Y coordinates of each impact location, the sheet in which the fragment is recovered and the fragment mass should be recorded. This information combined with an impact speed versus depth of penetration expression, and an air drag expression can be used to determine initial fragment masses and velocities. The depth of penetration and air drag expressions should be generated by single fragment firings if necessary.

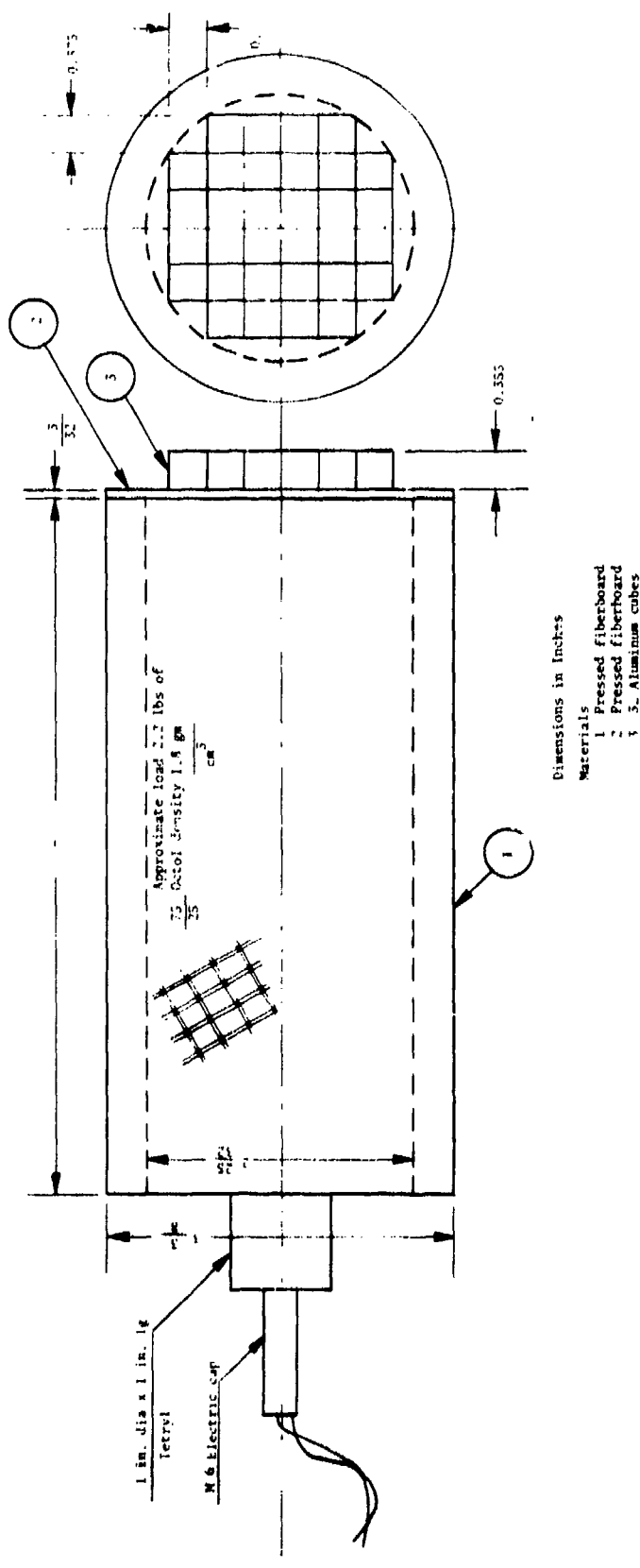


Figure 1. End Projector

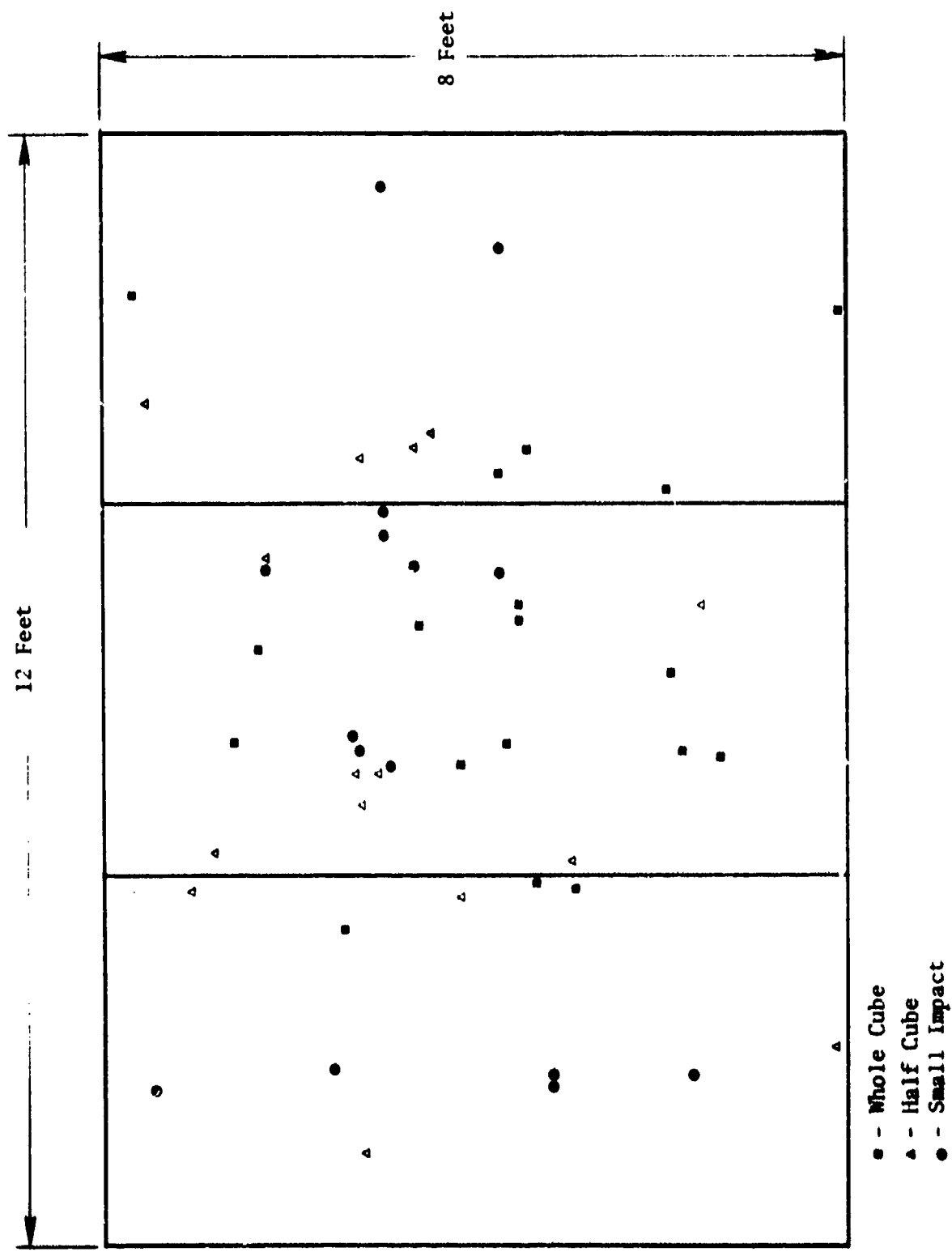


Figure 2. Fragment Spatial Distribution at 24 Feet

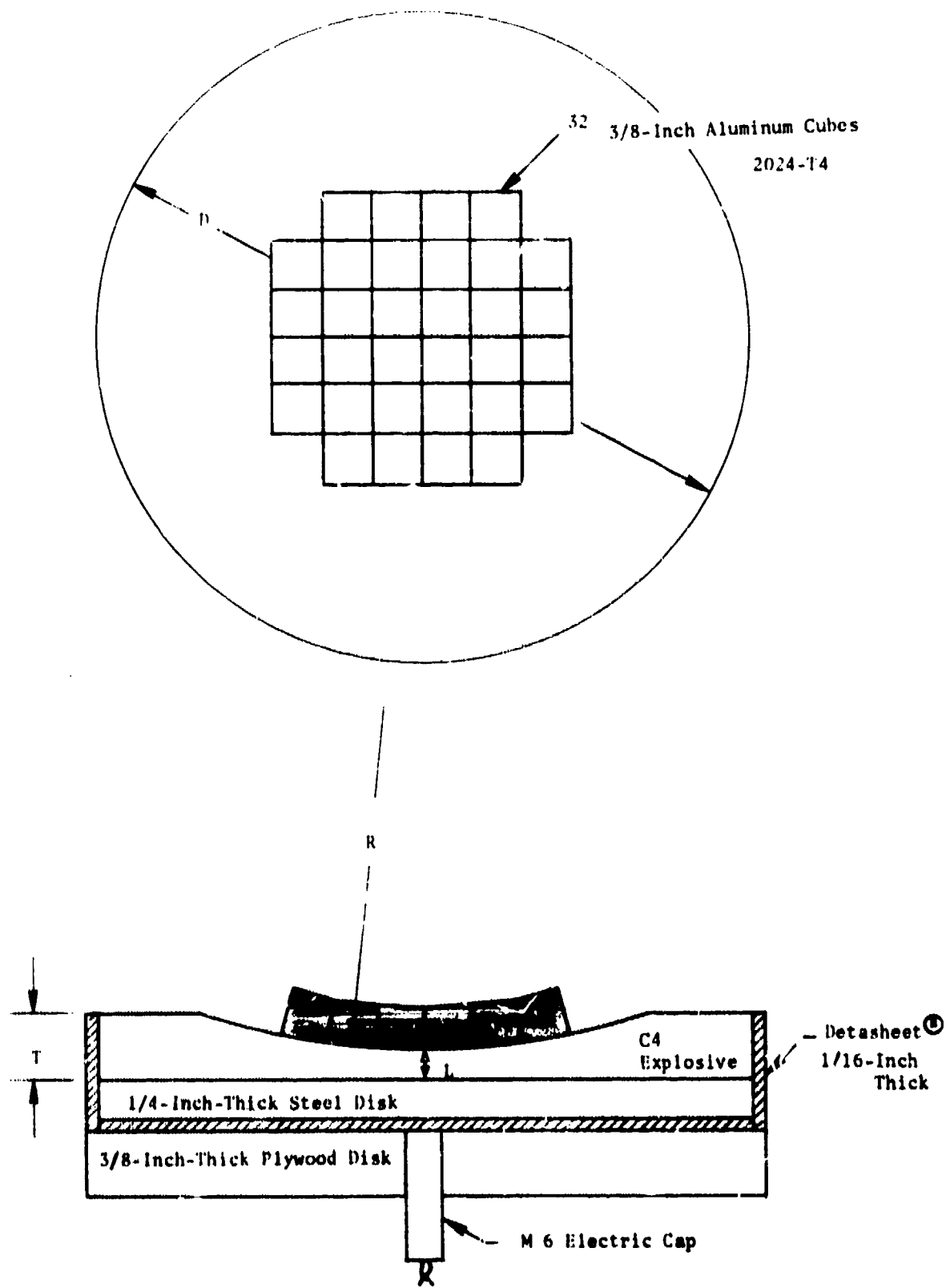


Figure 3. Dished Mat Projector

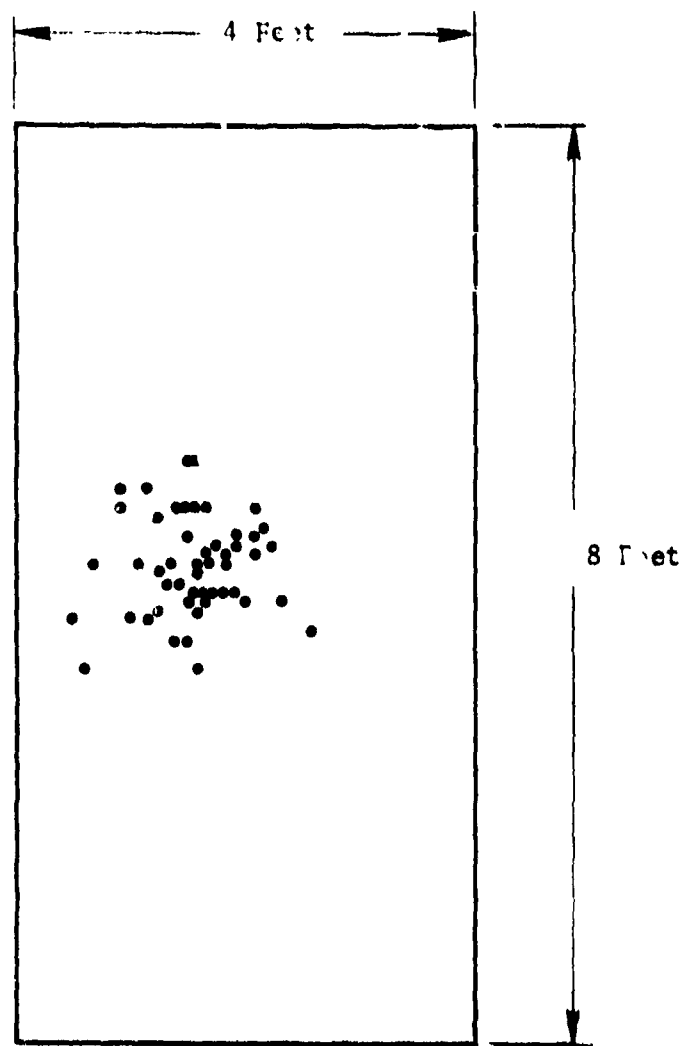


Figure 4. Witness Panel Impacts at 24 Feet, Shot Number 30

32, 3/8-Inch Aluminum Cubes
2024-T4

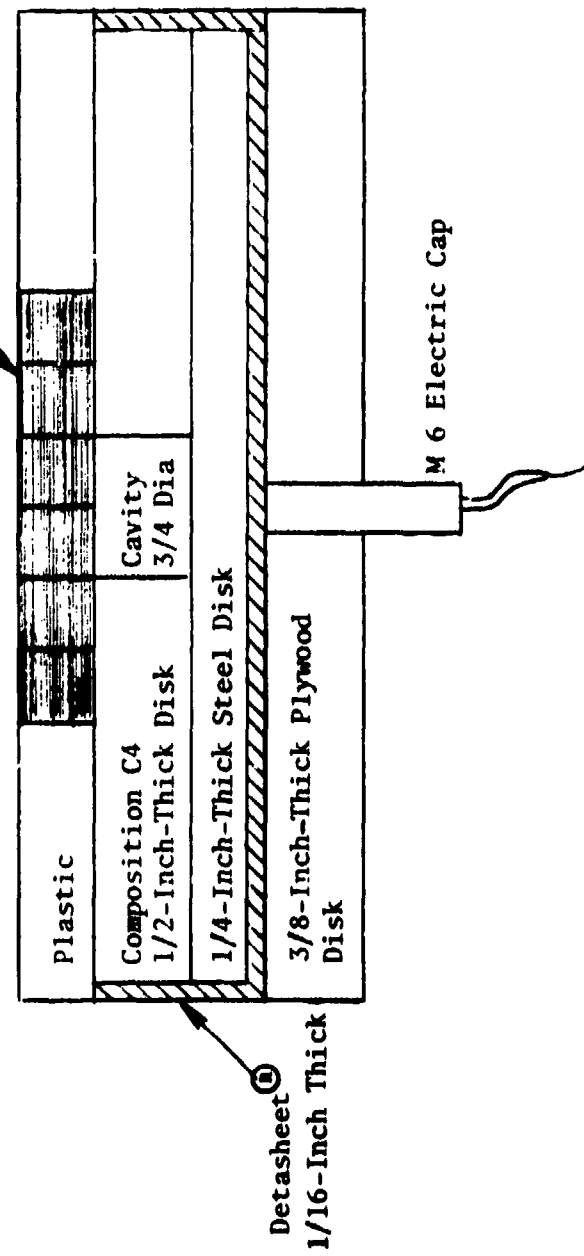


Figure 5. Cross Section of Plastic Filled Mat Projector

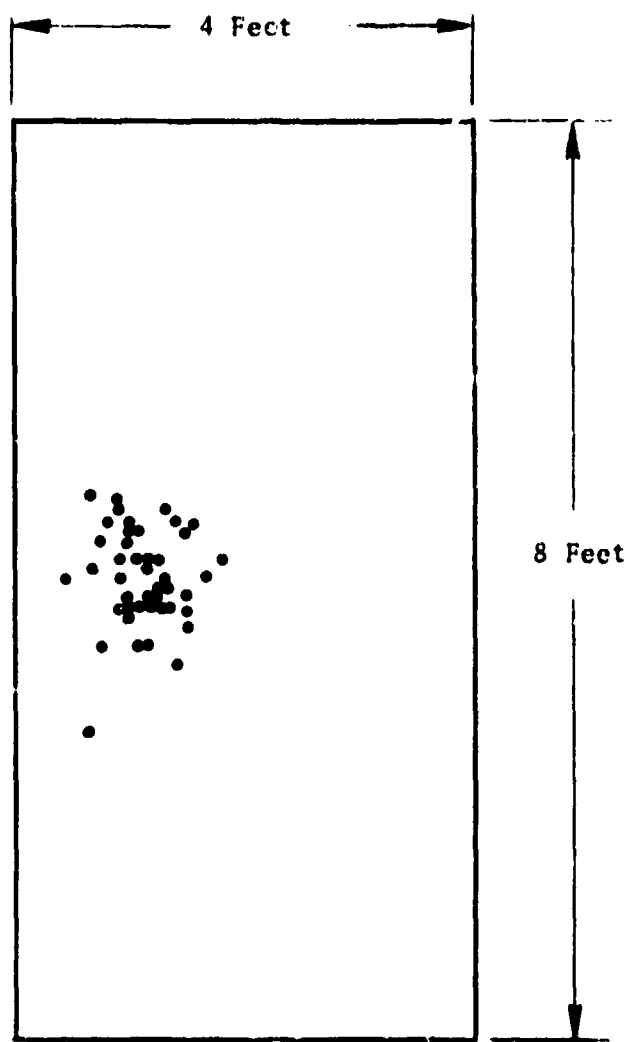


Figure 6. Witness Panel Impacts at 24 Feet, Shot 44

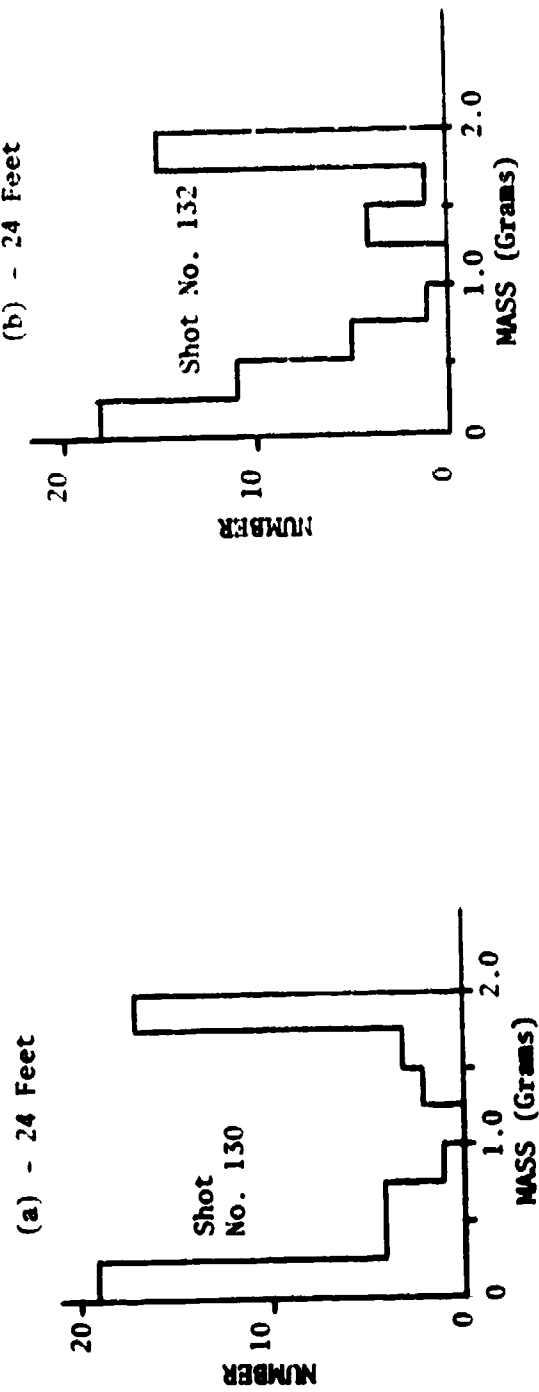


Figure 7. Number of Recovered Fragments by Mass Class

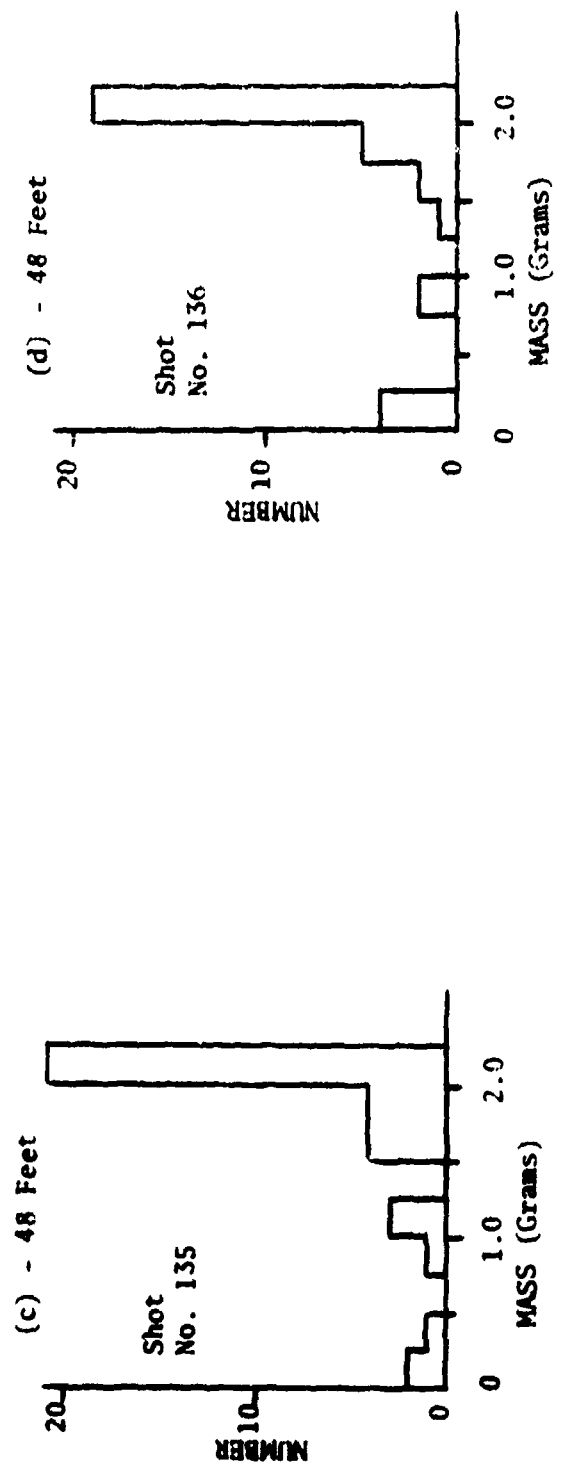


Figure 7. Number of Recovered Fragments by Mass Class (Continued)

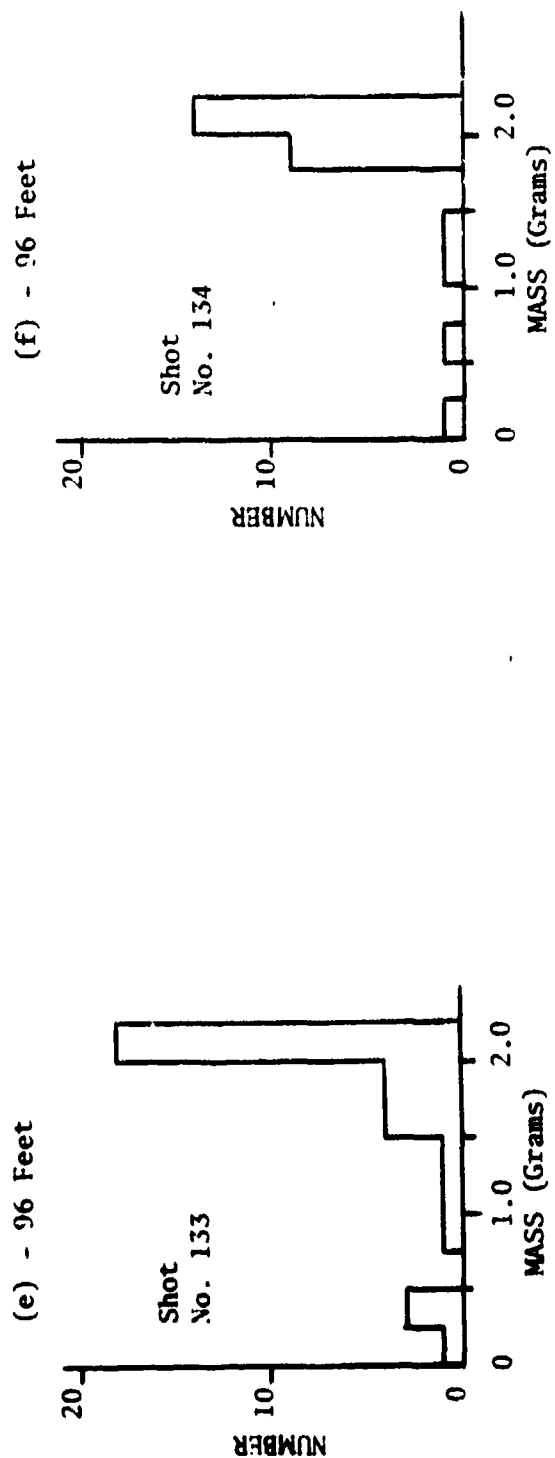


Figure 7. Number of Recovered Fragments by Mass Class (Concluded)

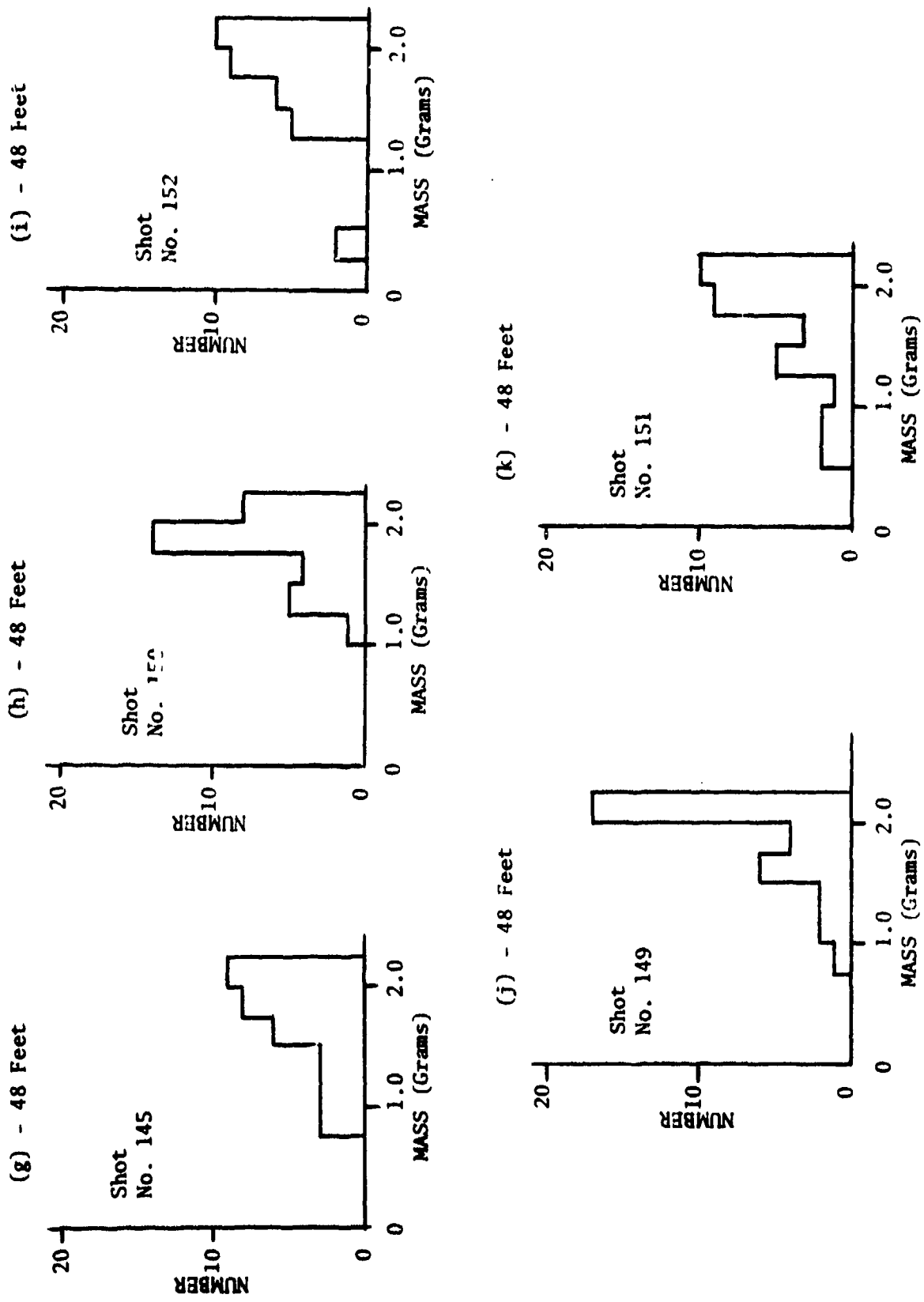


Figure 8. Number of Recovered Fragments at 48 Feet by Mass Class

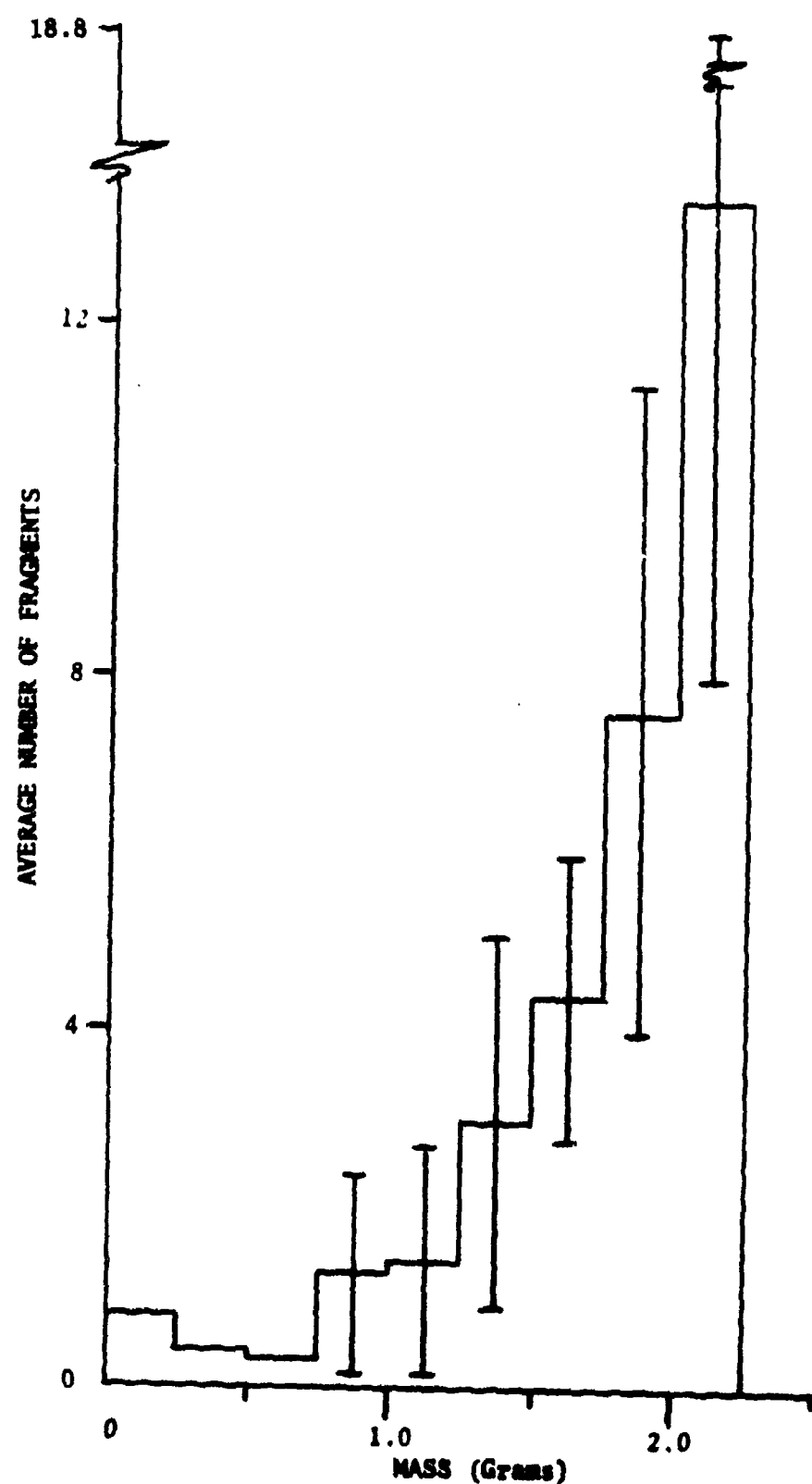
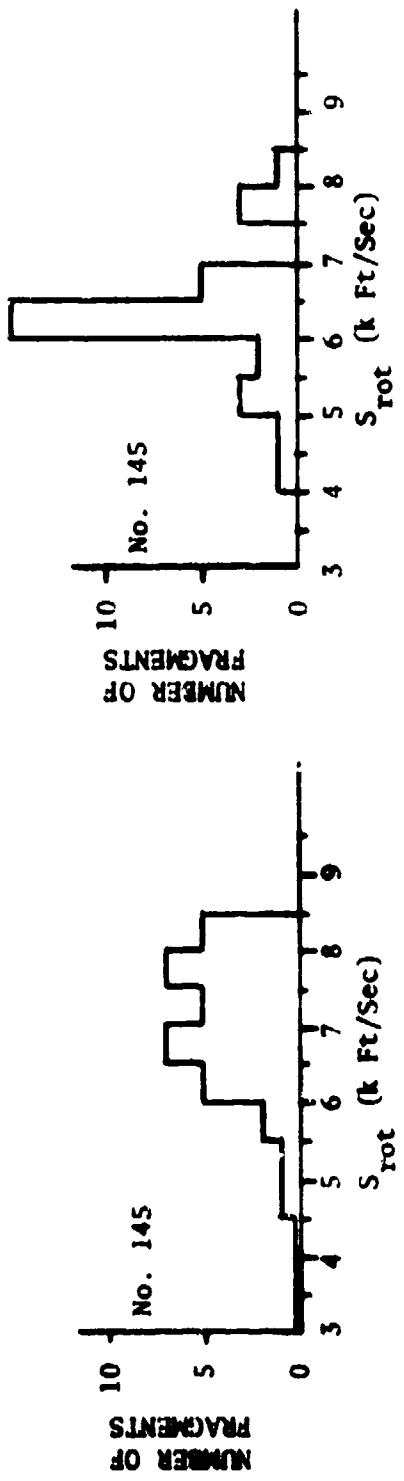


Figure 9. Average Number of Fragments at 48 Feet by Mass Class

DAHlgREN SCREENS

DEPTH OF PENETRATION



DAHlgREN SCREENS

DEPTH OF PENETRATION

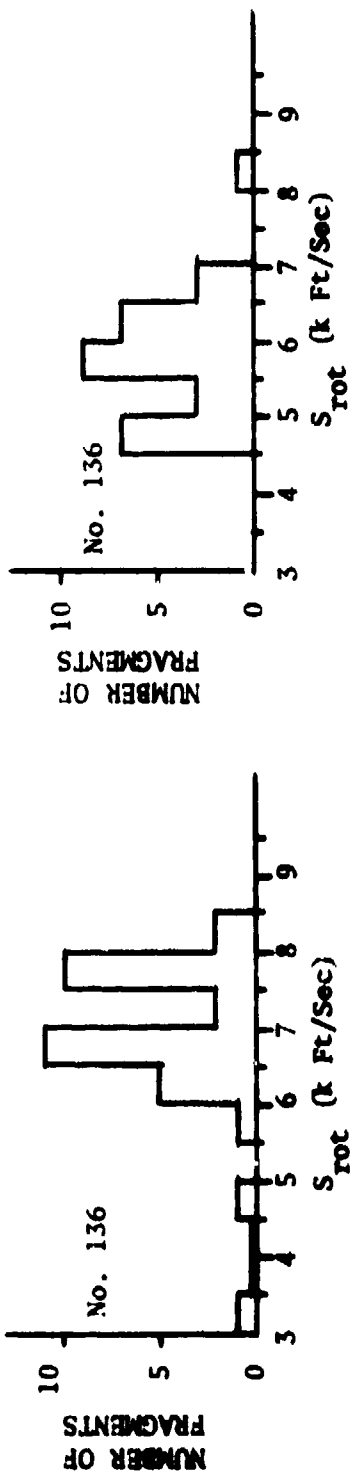


Figure 10. Comparison of Speed Measurement Techniques

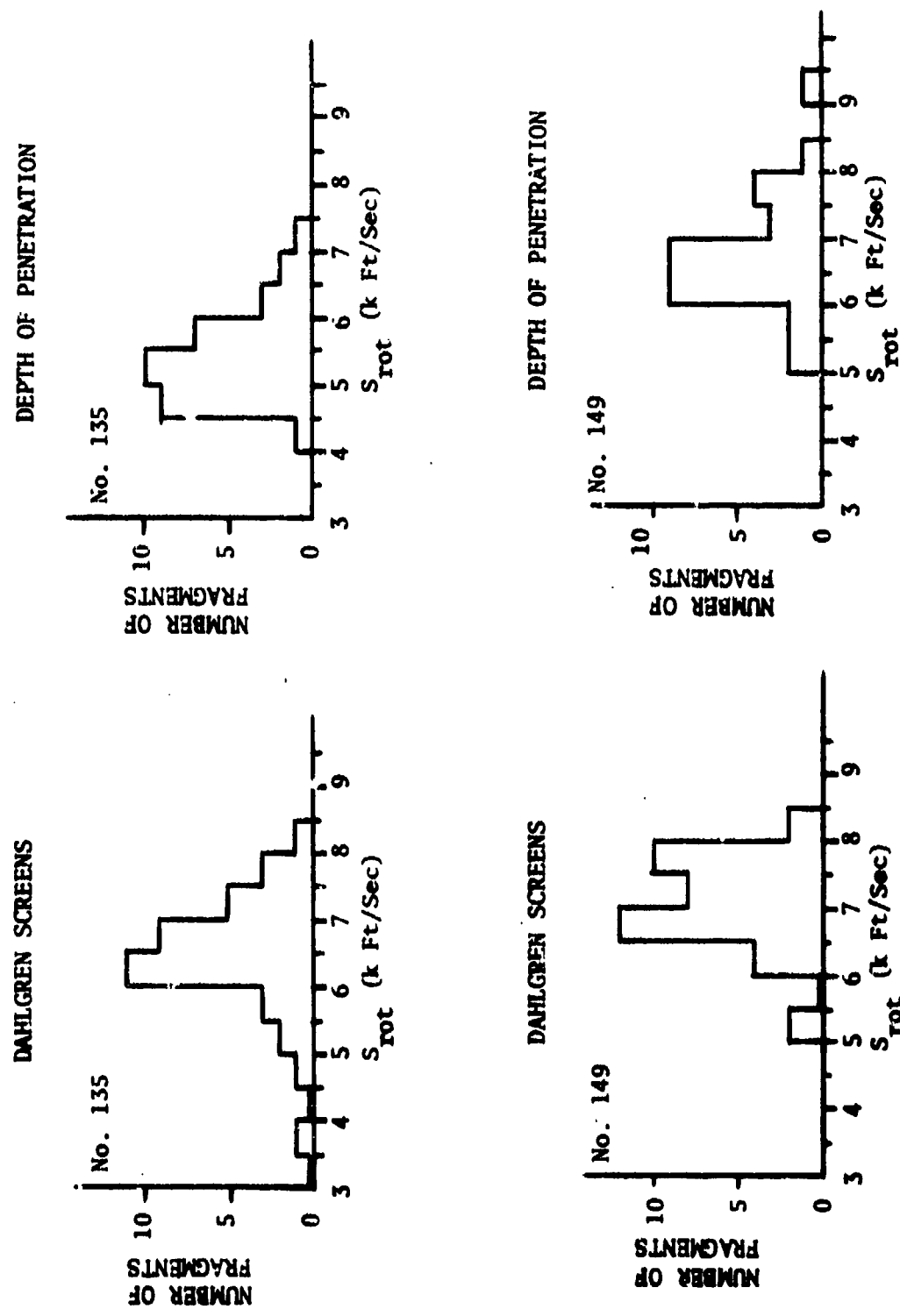


Figure 10. Comparison of Speed Measurement Techniques (Continued)

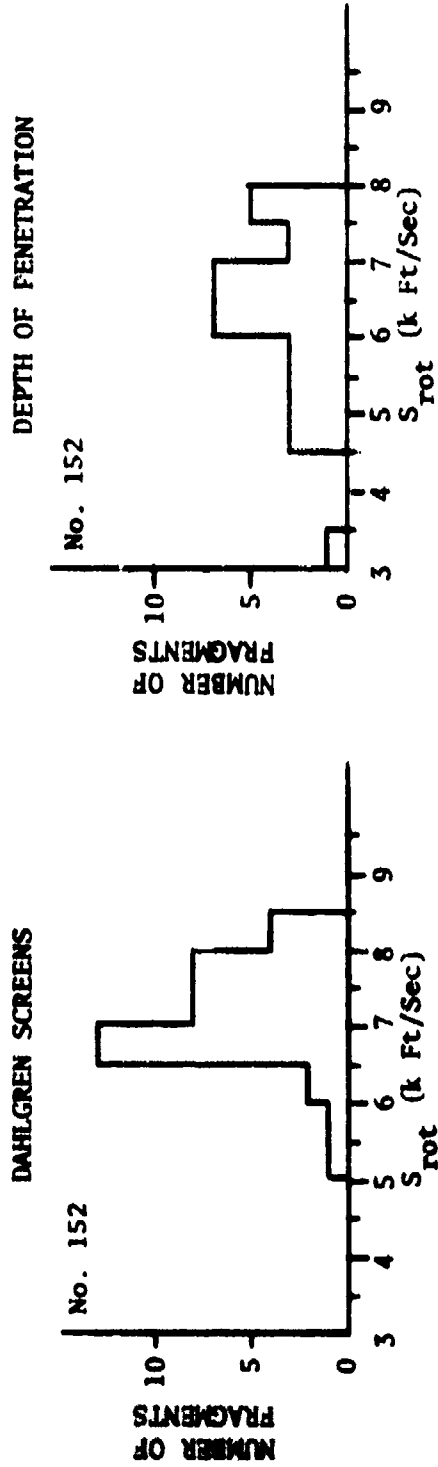


Figure 10. Comparison of Speed Measurement Techniques (Concluded)

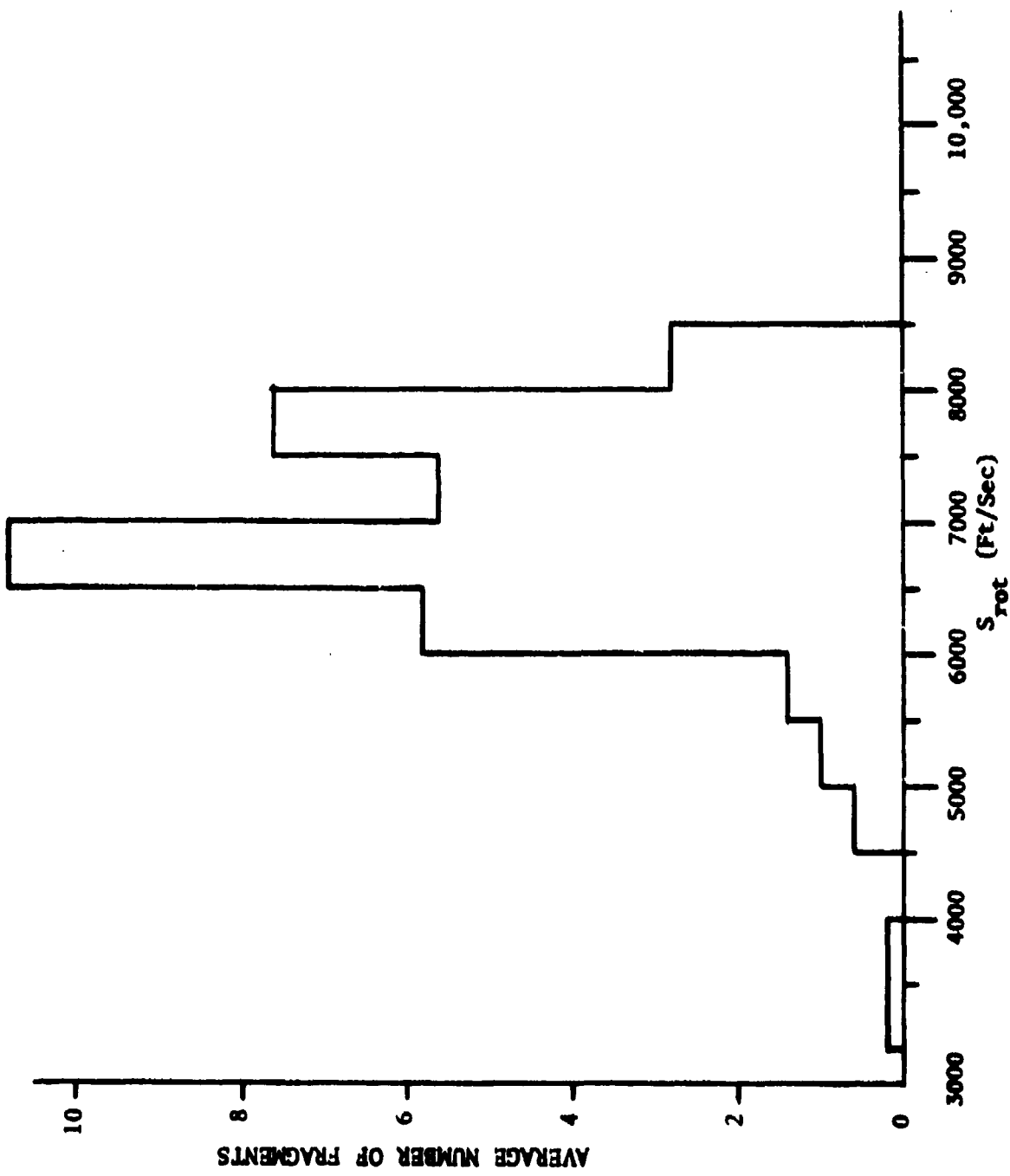


Figure 11. S_{rot} Distribution by Dahlgren Screens

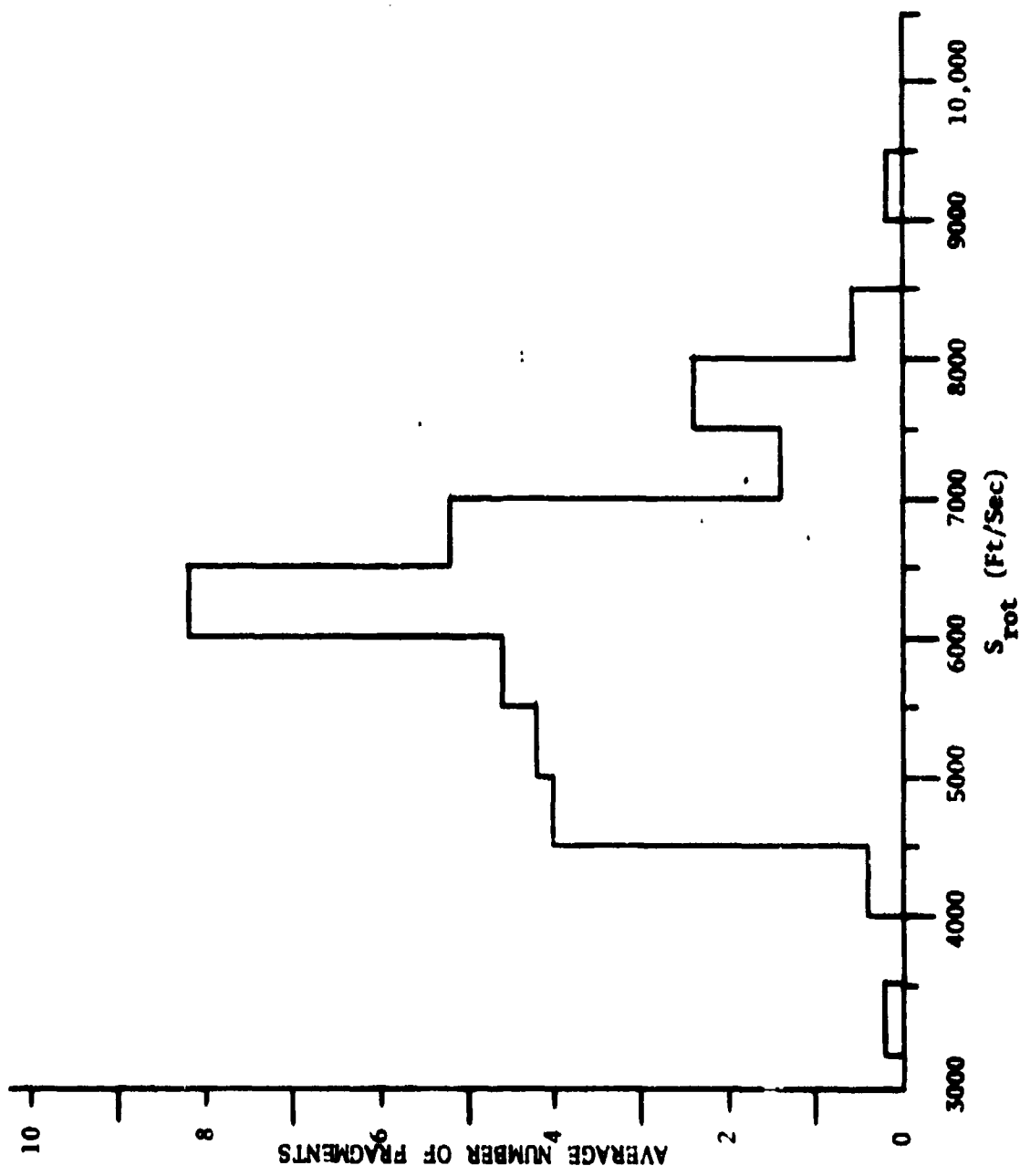


Figure 12. S_{rot} Distribution by Depth of Penetration

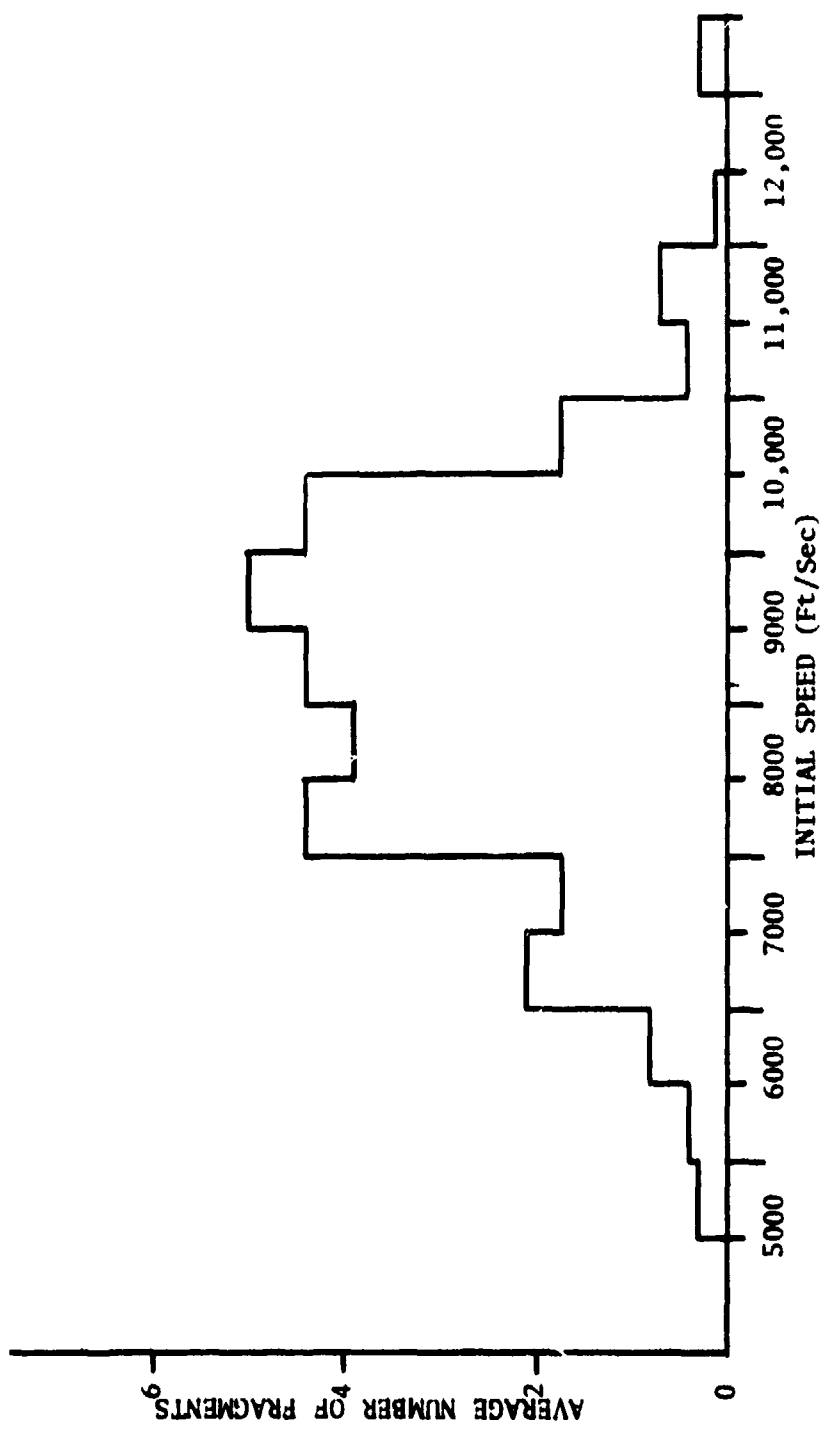


Figure 13. Initial Speed Distribution by Depth of Penetration

6 14x36-Inch Film Cassettes
13 Feet from X-Ray Head

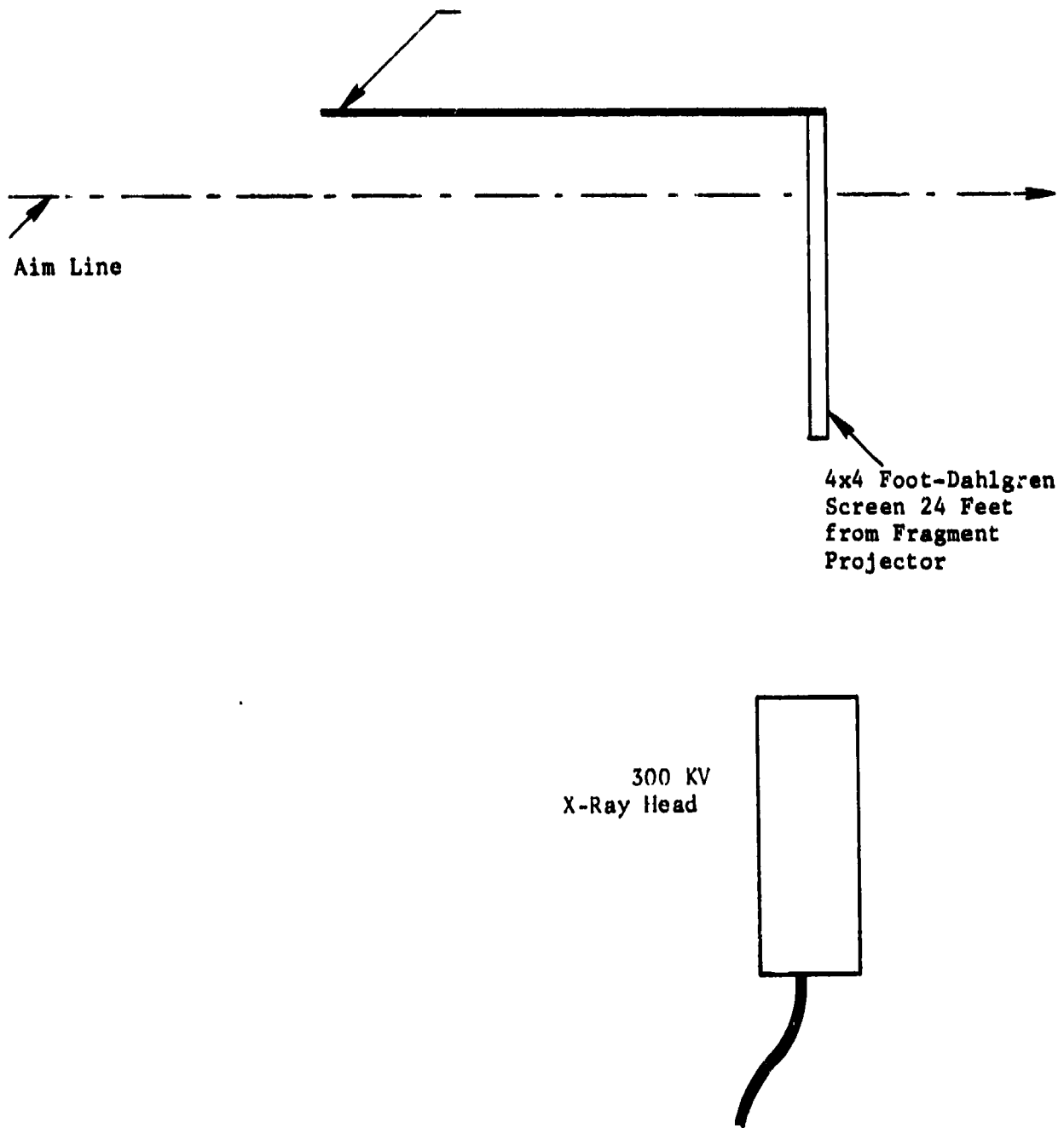


Figure 14. Plan View of X-Ray Set up

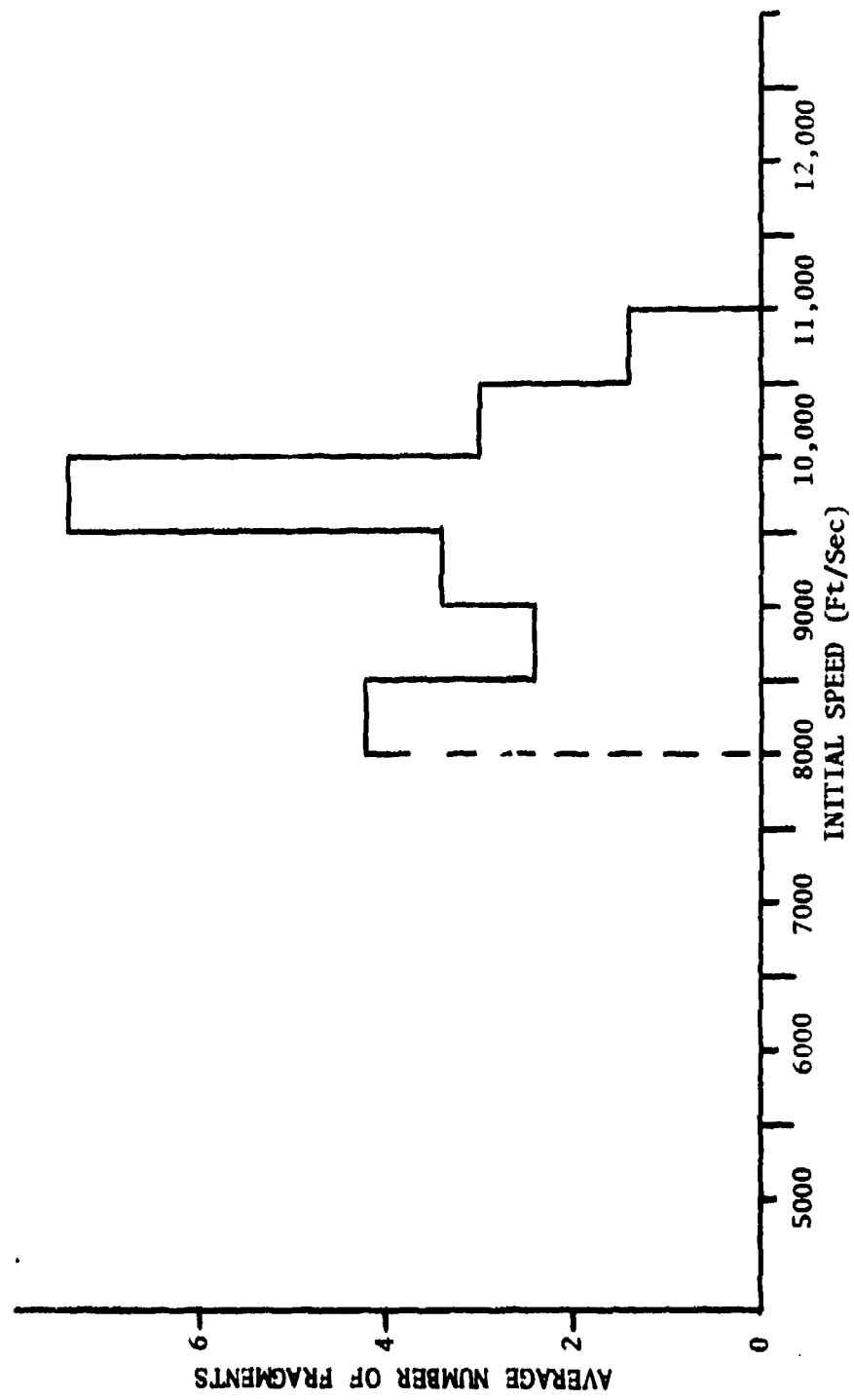


Figure 15. Initial Speed Distribution by Flash X-ray

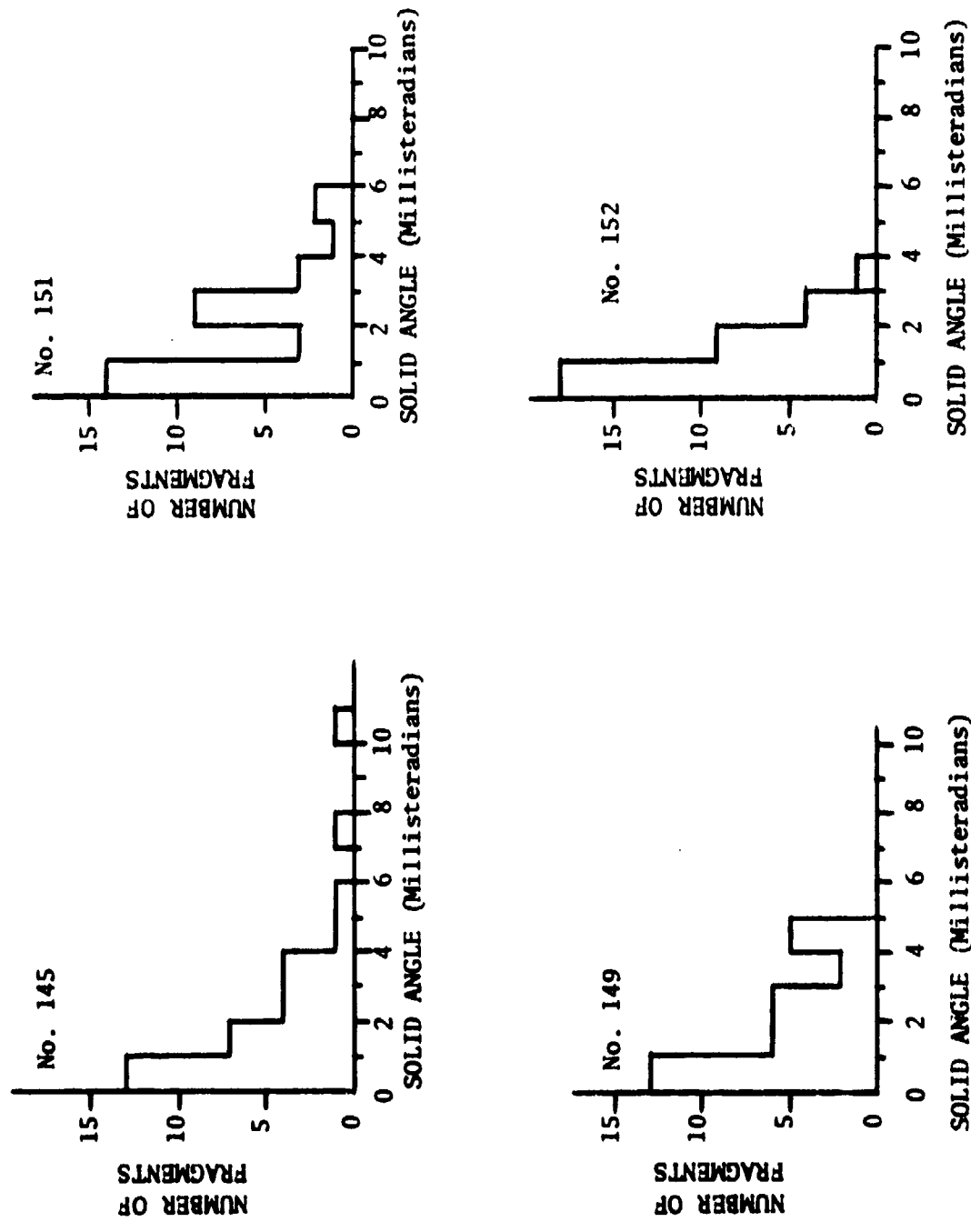


Figure 16. Fragment Spatial Distributions

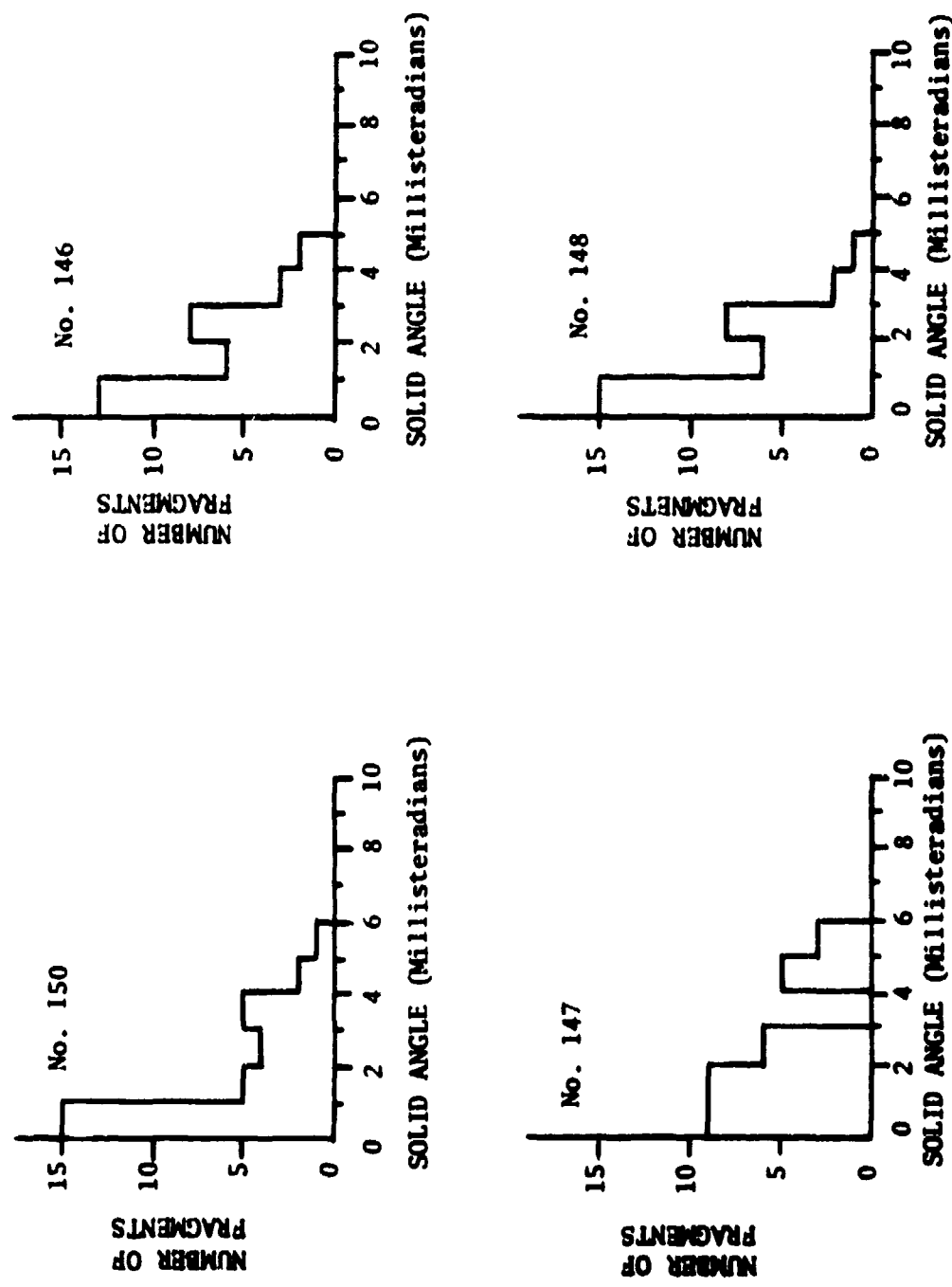


Figure 16. Fragment Spatial Distributions (Concluded)

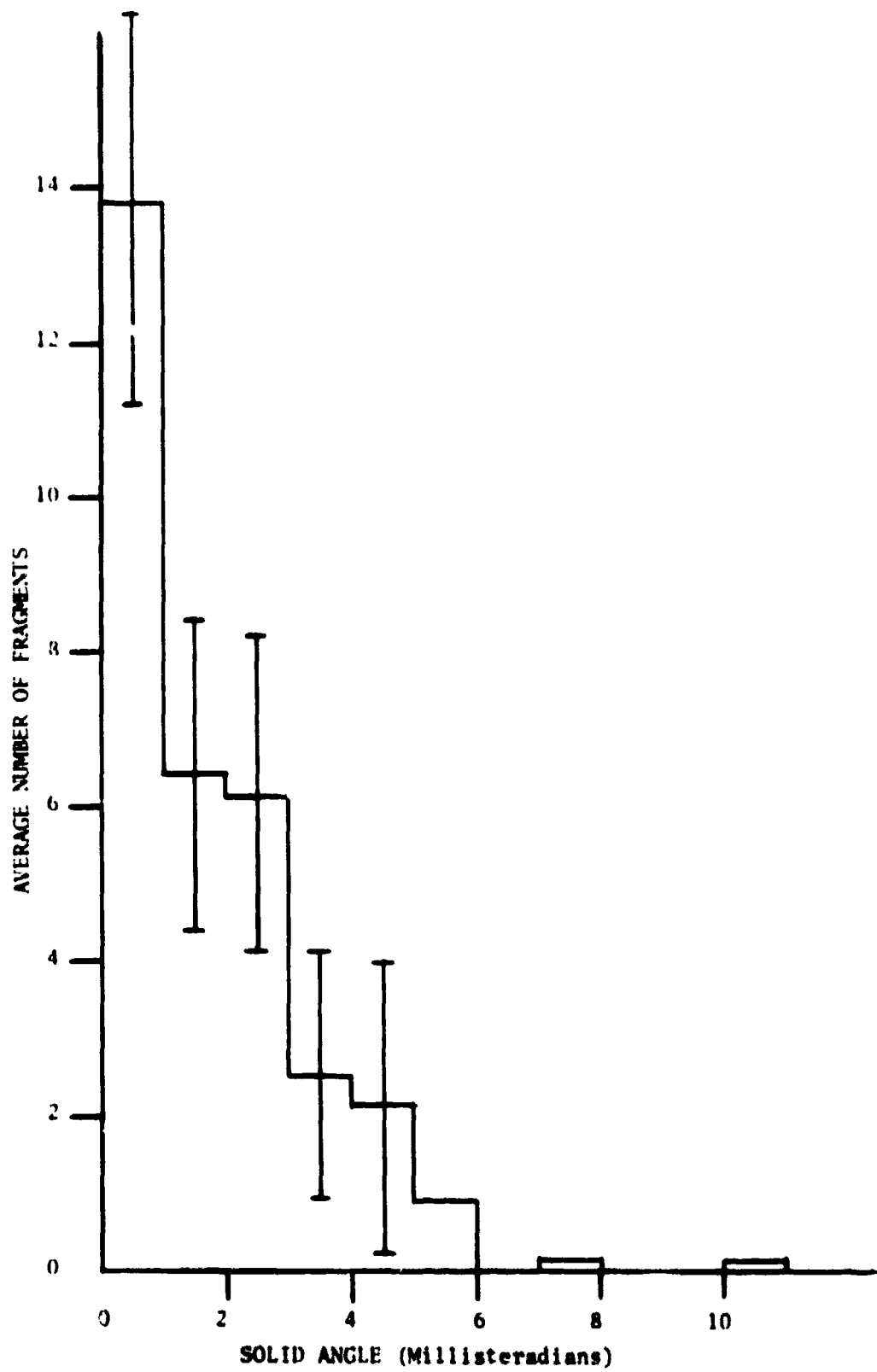


Figure 17. Average Fragment Spatial Distribution

TABLE 1. DISHED MAT PROJECTOR RESULTS

Shot Number	D Inches	R Inches	T Inch	L Inch	Composition C4 Mass (Grams)	Datasheet Mass (Grams)	Initial Speed Ft/Sec	^a Ω_{75} (Millisteradians)	Number of Impacts
30	5	3.5	1/2	NM	225	55	8125	2.9	49
32	4	3.5	1/2	NM	178	25	5680	2.7	31
33	7	3.5	1/2	NM	502	98	7775	3.9	54
34	5	3	1/2	1/8	277	60	8125	2.3	34
35	5	3	5/8	0	274	60	7775	0.9	37
b36	5	3	1/2	1/8	281	60	9000	157.6	29
37	5	3	1/2	1/8	270	60	8475	6.7	27
38	7	NM	1/2	3/16	529	98	7800	27.0	34
39	7	NM	1/2	1/16	492	98	6725	4.1	32
40	5	NM	1/2	3/16	218	52	6750	25.8	30
41	5	7	1/2	1/8	238	55	6600	7.0	32

^aSolid angle about the center of impact that includes 75 percent of the impacts.

bThe cubes for this shot were not placed in the concave surface of the explosive, but were in the plane parallel to the front surface.

NM Not measured

TABLE 2. PROPERTIES OF ALUMINUM FILLED PLASTIC

Hardeners Number	Density Grams/cc	Compressive Strength PSI		Flexural Strength PSI		Tensile Strength PSI
		Ultimate	Module	Ultimate	Module	
927	1.74	26,000	720,000	14,000	1.2×10^6	7000

TABLE 3. DESIGN PARAMETERS AND RESULTS

Shot Number	Explosive Thickness (Inch)	Composition C4 Mass (Grams)	Detasheet Mass (Grams)	① Four Cubes In Center	Diameter of Cavity (Inches)	Maximum Initial Speed (Ft/Sec)	Number Of Impacts	Ω_{75} (Millisteradians)	Avg. Recovered Fragment Mass (Grams)
43	0.50	284	54	No	0.75	7550 ^a	26	2.6	1.600
44	0.50	279	54	No	0.75	7700 ^a	27	3.4	1.759
46	0.50	270	54	No	0.75	7725	33	2.8	1.892
47	0.50	273	54	No	0.75	7700	39	1.8	1.706
49	0.50	284	54	Yes	0.75	7375	31	4.9	1.924
50	0.50	289	54	Yes	0.75	7400	25	3.3	1.934
51	0.50	289	54	No	0.0	8250	27	3.3	2.084
52	0.50	289	54	No	0.0	8250	33	3.7	1.957
53	0.50	289	53	Yes	0.0	8750	28	9.1	2.014
54	0.50	290	51	Yes	0.0	8825	28	3.6	1.832
56	0.75	388	57	Yes	0.75	8950	32	4.5	1.463
59	0.75	387	61	Yes	1.25	8425	34	5.2	1.070
55	0.75	401	57	Yes	0.0	11,300	19	5.4	1.915
65	0.75	408	59	Yes	0.0	9775	35	2.9	1.463
67	0.75	391	61	Yes	0.0	8850	26	1.7	1.748
64	1.0	535	67	Yes	0.75	9475	34	4.2	1.227
68	1.0	546	68	Yes	0.75	9500	20	1.7	1.312
63	1.0	564	72	Yes	0.0	11,475	NR	NR	NR
66	1.0	550	66	Yes	0.0	11,225	48	2.2	1.067

^aBased on flash panel impact at 24 feet.

^bSolid angle about the center of impact that includes 75 percent of the impacts.

NR Not recorded.

TABLE 4. FINAL DESIGN PERFORMANCE

Shot Number	Speed Determination Method	Standoff Distance (Feet)	Composition C4 Detonate Mass (Grams)	Initial Speed (Ft/Sec)	C-5 Mass (Milli-steradians)	Fragments With Mass Greater Than 0.25 Grams			All Fragments		
						Average Recovered Fragment Mass (Grams)	Number of Recovered Fragments	Total Mass (Grams)	Number of Velocity Signals	Number of Fragments	Total Mass (Grams)
66	DS	24	550	67	11,225	1.5	1.03	31	14	34	31.4
130	DS	24	NR	NR	10,550	NR	1.44	31	14	50	4.1
132	DS	24	NR	NR	11,625	NR	1.18	37	14	55	45.9
141	X-RAY	24	96	NR	11,025	NR	NA	NA	30	34	NA
110	X-RAY	24	96	NR	10,700	NR	NA	NA	30	34	NA
111	X-RAY	24	96	NR	10,550	NR	NA	NA	23	34	NA
114	X-RAY	24	96	NR	10,900	NR	NA	NA	31	34	NA
115	X-RAY	24	96	NR	10,725	NR	NA	NA	34	34	NA
116	X-RAY	24	96	NR	11,200	NR	1.68	34	36	42	65.9
135	DS	48	NR	NR	11,525	NR	1.84	30	35	39	58.1
136	DS	48	NR	NR	11,400	2.6	1.72	31	33	35	54.1
145	DS	48	538	64	11,000	2.9	1.62	32	36	38	56.3
149	DS	48	537	62	90	5.0	1.82	32	58.2	32	58.1
150	DS	48	527	62	90	5.0	1.82	32	52.5	32	52.5
151	DS	48	504	67	12,175	2.6	1.64	32	1.4	32	55.3
152	DS	48	512	68	11,500	1.3	1.73	32	55.3	32	55.3
146	FP	48	550	65	NR	2.5	NA	NA	ND	32	NA
147	FP	48	532	63	NR	2.7	NA	NA	ND	32	NA
148	FP	48	550	63	NR	2.6	NA	NA	ND	32	NA
133	DS	96	NR	NR	11,850	NR	1.83	32	11b	33	55.5
134	DS	96	NR	NR	12,025	NR	2.02	27	54.0	28	54.5

aOnly first arrival recorded

bOnly one 4 x 4 foot Dahlgren screen used

FP = Flash Panel
NA = Not applicable
NR = Not recorded
DS = Dahlgren screen

REFERENCES

1. Shelley, Sidney O., Vulnerability and Lethality Testing System (VALTS),
Armament Development and Test Center Report ADTC-TR-72-127,
December 1972, Unclassified.

APPENDIX A
COMPUTATION METHODS

This appendix lists the relationships used to convert the measured data into more convenient and usable forms.

1. AERODYNAMIC DRAG EXPRESSIONS

Given that a fragment had an initial speed S_0 , the speed after it has traveled a distance x , is given by

$$S = S_0 e^{-\alpha x} \quad (1)$$

where α is a constant given by

$$\alpha = \frac{C_d \rho A}{2m} \quad (2)$$

The quantities in this expression are defined as

C_d aerodynamic coefficient of drag

ρ air density

A fragment presented area

m fragment mass

While sufficient information is available to determine α for new, unfired, whole cubes, none is available for the distorted, partial fragments typical of this projector. Therefore a series of Mann barrel firings was conducted to determine the effective α for actual fragments. The results are:

(3a) 0.25 grams $\leq m < 0.75$ grams	$\alpha = 0.0200/\text{ft}$
(3b) 0.75 grams $\leq m < 1.25$ grams	$\alpha = 0.0153/\text{ft}$
(3c) 1.25 grams $\leq m < 1.75$ grams	$\alpha = 0.0137/\text{ft}$
(3d) 1.75 grams $\leq m \leq 2.26$ grams	$\alpha = 0.0129/\text{ft}$

(3)

Equation (1) was used in the form

$$S_0 = S e^{\alpha x} \quad (4)$$

to calculate initial speeds from impact speeds in the case of the fragments recovered from fiberboard.

In order to calculate the quantity S_{rot} from impact speeds, an expression relating impact speeds and arrival times is required. The first integral of Equation (1) provides such an expression.

$$S = S_0 e^{-\alpha x} \quad (1)$$

as

$$\frac{dx}{dt} = S \quad (5)$$

substituting for S and integrating

$$\begin{aligned} x &= R & t &= T \\ \int e^{\alpha x} dx &= \int S_0 dt \\ x &= 0 & t &= 0 \end{aligned} \quad (6)$$

where T is the arrival time of the fragment at the distance $x = R$.

$$T = \frac{\{e^{\alpha R} - 1\}}{\alpha S_0} \quad (7)$$

or

$$T = \frac{\{1 - e^{-\alpha R}\}}{\alpha S} \quad (8)$$

where S is the speed of the fragment after it has traveled a distance R.

The quantity S_{rot} is:

$$S_{rot} = \frac{R}{T} \quad (9)$$

Substituting for T, this becomes

$$S_{rot} = \frac{\alpha R S}{\{1 - e^{-\alpha R}\}} \quad (10)$$

This expression was used to calculate S_{rot} from speed data obtained at 48 feet.

Equation (7) can be solved for S_o to give

$$S_o = \frac{\{ e^{\alpha R} - 1 \}}{\alpha T} \quad (11)$$

Equation (11), along with an assumption regarding the value of α , can be used to calculate initial speeds from Dahlgren screen, flash panel, or other time of arrival data.

2. DEPTH OF PENETRATION RELATION

Aluminum fragments recovered during the course of the development tests were fired singly from a Mann barrel into fiberboard at impact speeds up to 5000 ft/sec. From the recovered fragment masses and depths of penetration the following relationships were established:

$$S_{DOP} = C \cdot N \quad (12)$$

where

S_{DOP} is the impact speed and N is the number of the fiberboard sheet from which the fragment is recovered

and

(13a) 0.25 grams \leq m < 0.75 grams	C = 482
(13b) 0.75 grams \leq m < 1.25 grams	C = 356
(13c) 1.25 grams \leq m < 1.75 grams	C = 278
(13d) 1.75 grams \leq m \leq 2.26 grams	C = 280

(13)

INITIAL DISTRIBUTION

Hq USAF/RDQ	1	USABRL/APG	1
Hq USAF/SAMI	1	ASD/ENFEA	1
OASD/SA	1	ADTC/SD-22	1
DIA/DIR-4C3	1	ADTC/SD-15	1
OSD/PA&E	1	ADTC/SD-3	1
AFIS/INTA	1	ADTC/SD-23	1
AFSC/XRPA	1	ADTC/SD-102	10
AFSC/SDW	1	AFATL/DLYV	1
TAC/XPSY	1	USAFTFWC/OA	
TAC/DRFA	1		
TAC/DOV	1		
TAC/DRA	1		
AFFDL/PTS	1		
ASD/XRL	1		
AFAL/RW	1		
ASD/ENYEHM	1		
AUL/LSE-70-239	1		
USAFTFWC/TE	1		
Hq SAC/XOB	1		
Hq SAC/NRI	1		
DDC	12		
US NAV WPNS CEN/Code 12	1		
US NAV WPNS CEN/Code 408	1		
US NAV WPNS CEN/Code 407	1		
USAF/AFSC/Code 143	1		
OGDEN ALC/MMNOP	2		
AFWL/LK	2		
AFATL/DLOSL	2		
AFATL/DL	1		
AFATL/DLJ	1		
AFATL/DLJF	1		
AFATL/DLJM	1		
AFATL/DLJK	1		
AFATL/DLJW	1		
AFATL/DLDG	1		
AFATL/DLD	1		
AFATL/DLY	1		
ADTC/XR	1		
ADTC/SD	1		
ADTC/INH	1		
SACPO	1		
TAWC/OA	1		
TAWC/TRAOCLO	1		
AFFDL/FES	2		